INTERNATIONAL ATOMIC ENERGY AGENCY
UNITED NATIONS EDUCATIONAL, SCIENTIFIC AND CULTURAL ORGANIZATION

INTERNATIONAL CENTRE FOR THEORETICAL PHYSICS
34100 TRIESTE (ITALY) - P.O.B. 586 - MIRAMARE - STRADA COSTIERA 11 - TELEPHONE: 2240-1
CABLE: CENTRATOM - TELEX 460392 - I

H4.SMR/285 - 29

WINTER COLLEGE ON
LASER PHYSICS: SEMICONDUCTOR LASERS
AND INTEGRATED OPTICS

(22 February - 11 March 1988)

# STRUCTURAL CHARACTERIZATION OF PROTON EXCHANGED $LiNbO_3$ OPTICAL WAVEGUIDES

R.M. De La Rue
Glasgow University
Glasgow, U.K.

# Structural characterization of proton exchanged $LiNbO_3$ optical waveguides

C. Canali
*Istituto di Elettrotecnica e di Elettronica, Via Gradenigo 6/A, 35131 Padova, Italy*

A. Carnera, G. Della Mea, and P. Mazzoldi
*Dipartimento di Fisica, Via Marzolo 8, 35100 Padova, Italy*

S. M. Al Shukri, A. C. G. Nutt, and R. M. De La Rue
*Department of Electronics and Electrical Engineering, University of Glasgow, Glasgow G12 8QQ, Scotland, United Kingdom*

(Received 16 September 1985; accepted for publication 18 December 1985)

This paper reports the results of structural analysis of proton-exchanged lithium niobate optical waveguides fabricated in *Z*-, *X*-, and *Y*-cut substrates immersed in pure benzoic acid. Rutherford backscattering spectrometry, nuclear reactions, secondary ion mass spectrometry, scanning electron microscopy, and x-ray diffraction were used to measure atomic composition profiles and the marked lattice distortion induced by the proton exchange process in the waveguiding layer. H and Li concentration measurements indicate an exchange of about 70% of the Li atoms are present in the virgin $LiNbO_3$ crystal.

## I. INTRODUCTION

The emergence of the proton exchange technique for optical waveguide fabrication[1] could have a major impact on the use of lithium niobate ($LiNbO_3$) in various applications of integrated optics. Proton exchange in $LiNbO_3$ is a low-temperature process which creates an increase ($\cong 0.12$ at $\lambda = 0.633\ \mu m$) in the extraordinary refractive index larger than that produced by conventional Ti in-diffusion ($< 0.02$ at the same wavelength).[1-4] Several devices have already demonstrated, e.g.: grating beam splitters,[5] Fresnel lenses,[6] polarization strippers,[7] modulators,[8] and birefringence controllers.[9] Proton exchange also shows the additional advantage of decreasing the susceptibility to optical damage (the photorefractive effect)[10] so that devices made by proton exchange can operate using higher powers of shorter wavelengths than devices based on Ti in-diffused optical waveguides.

Some important practical problems have been identified in proton exchanged waveguides. In particular the low temperature at which the exchange takes place has led to concern about long term or thermal stability of the guides.[11] Furthermore, the high hydrogen concentration introduced into the host lattice may induce large crystal distortions and the surface damage observed in *Y*-cut substrates[1,12,13] and/or the formation of new phases resulting in highly scattering guides[2,14] and in a deterioration in the electro-optic and acousto-optic properties.[15]

Several papers report the optical properties of proton exchanged (PE) waveguides but very little fundamental or systematic research on the proton-lithium exchange process in $LiNbO_3$ has been carried out. For example, Li and H concentrations and profiles have not been directly measured except as reported in Ref. 16, where preliminary measurements of hydrogen profiles are given; x-ray diffraction methods have not been used to determine strains or defects in the exchanged layer; a new crystalline phase ($HNbO_3$) with a cubic perovskite structure was detected in x-ray diffraction studies of $LiNbO_3$ exchanged powders[17] but direct experimental evidence for its presence also in the exchanged $LiNbO_3$ single-crystals substrates has not been obtained.[12,17]

There is clearly a need to establish, unambiguously, the structural characteristics of waveguides formed by proton exchange in $LiNbO_3$ and their correlation with optical properties to give a basis for the design of well-controlled and reliable devices.

This paper is primarily concerned with structural analysis studies of proton-exchanged lithium niobate waveguides fabricated on crystalline substrates with different crystallographic orientations by immersion in pure molten benzoic acid at different exchange temperatures and for different exchange periods. Before structural analysis has been carried out the optical characteristics of the waveguides have been obtained using the standard prism-coupler technique. Strains, defects, and crystal structure modifications have been studied using x-ray diffraction methods, while Rutherford backscattering spectrometry (RBS) has been used to study the kinetics of waveguide formation and of the exchange process. H and Li concentrations and profiles have been estimated via nuclear reactions.

## II. SAMPLE REACTION

Optical-grade, polished, single-crystal $LiNbO_3$ substrates supplied by Barr and Stroud Ltd. were cleaned and degreased thoroughly using a series of organic solvents. The samples were then mounted in a PTFE holder before being placed in 250 ml of pure benzoic acid in a stainless-steel beaker placed in an oil bath the temperature of which was controlled to within $\pm 0.25$ °C. The benzoic acid was renewed after, at the most, 20 exchange runs. Both the oil bath and exchange beaker were covered to provide a well-isolated temperature-stable environment.

Exchange temperatures and times used ranged from 150 to 250 °C and from 20 min to a few hours, respectively. Sample preheating was used for shorter exchange periods. The exchange time was defined as that between immersion of the sample in the benzoic acid and its removal from the acid. Benzoic acid crystallized on cooled samples was removed by

 0021-8979/86/082643-07$02.40  

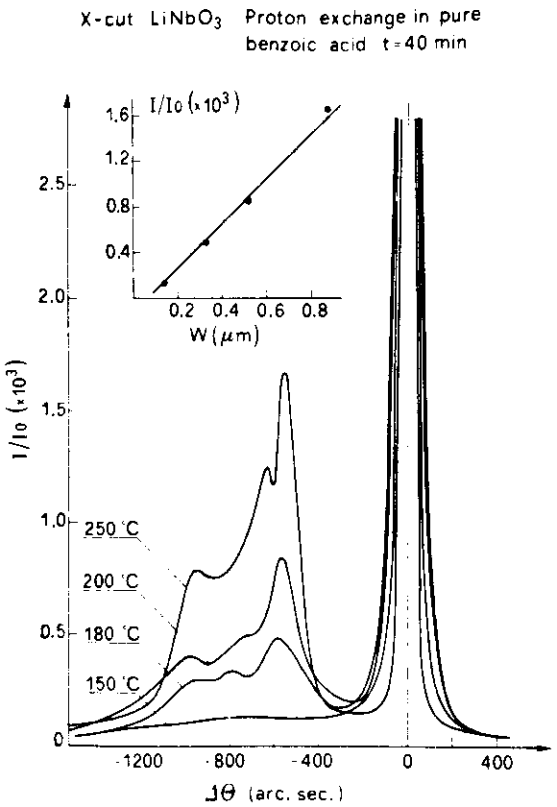


FIG. 1. Double-crystal x-ray diffraction, (220) rocking curves obtained on X-cut samples isochronally (40 min) exchanged at different temperatures in pure benzoic acid. The insert shows the dependence of the satellite peak amplitude on the thickness of the exchanged layer $W$.

chloroform and/or methanol. The samples were then stored for a long enough period for the refractive index of the waveguide region to relax to a stable value,[2,11] typically for at least two weeks.

## III. RESULTS AND DISCUSSIONS

### A. Optical characterization

The mode structure and propagation losses of the optical waveguides were measured by means of the conventional prism-coupler technique with single-crystal rutile prism[2] at $\lambda = 0.633\ \mu$m. The values of the effective refractive indices of each observed mode were used as the input for a computer program to calculate the refractive index profile and the depth of the planar waveguides. The obtained results agree with those previously reported in Refs. 2 and 18. In particular, the increase of the extrordinary refractive index showed a steplike profile with a maximum of about 0.126 for both $Z$- and $X$-cut substrates.

Propagation losses were measured by monitoring the out-of-plane scattering light, imaging it on an infrared vidicon, and displaying the amplitude of the scattered light signal.[2,18] Measured losses were between 2.5 and 6 dB/cm; similar propagation losses, as large as 6 dB/cm, were reported in Ref. 14, and, in both cases, the experimental values are much higher than values given by Jackel.[1]

### B. X-ray diffraction methods

Strains and crystal structure modifications induced by proton exchange have been studied by x-ray diffraction methods. In particular, a double-crystal diffractometer was used to measure strains present in the waveguide region and x-ray diffraction topography was used to detect defects. Glancing-angle x-ray diffraction was carried out in a Wallace–Ward cylindrical texture camera[19] to investigate the presence of new phases formed during the proton exchange process.

Figure 1 shows double-crystal x-ray diffraction, (220) rocking curves, taken on $X$-cut samples all exchanged for 40 min in pure benzoic acid at four different temperatures. The presence of satellite peaks at a negative deviation $\Delta\theta$ from the Bragg angle relative to the unperturbed substrate indicates that the exchanged layer exhibits a positive strain, $\Delta a/a > 0$ perpendicular to the surface. The shape and position of the satellite peaks remain the same with increasing the exchange temperature. Furthermore, as shown in the insert in Fig. 1, their intensity increases linearly as a function of the exchanged layer thickness. Even though an accurate evaluation of the lattice strain value and distribution requires theoretical simulation of the experimental rocking curves, inspection of the features of the spectra reported in Fig. 1 allows a qualitative estimate of about 0.8% for the strain present.

Positive strains perpendicular to the surface have also been observed to occur for similar treatments in $Z$- and $Y$-cut substrates and in particular, on $Y$-cut PE samples, strains as large as 1.6% have been observed. Furthermore, in these substrates when the exchanged layer thickness exceeds about 2000 Å a surface damage appears as reported by other authors.[1,12–14,20] This phenomenon is clearly evident in both scanning electron microscope (SEM) and x-ray topography (XRT) observations. Figure 2(a) is a low magnification SEM micrograph taken on a $Y$-cut sample proton exchanged for 20 min at 180 °C, showing a large number of cracks running along the $x$ axis. At higher magnification [Fig. 2(b)],

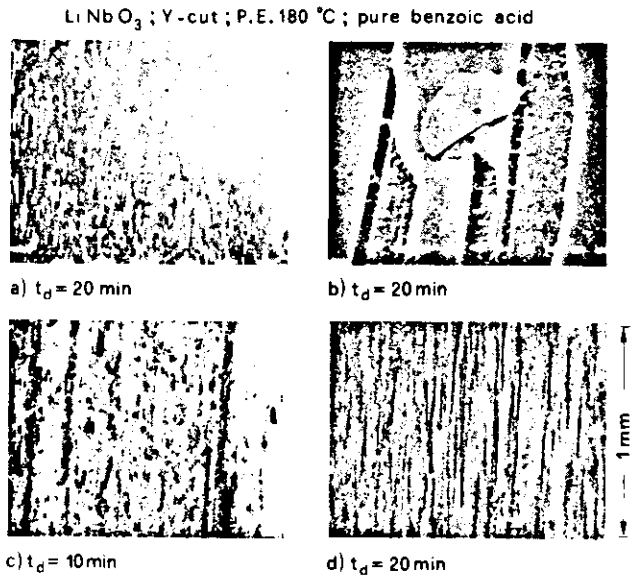


FIG. 2. (a) and (b) are SEM micrographs taken at two different magnifications [markers are 125 and 2 $\mu$m long in (a) and (b), respectively] on $Y$-cut samples exchanged at 180 °C for 20 min. (c) and (d) are x-ray topographs (Cu$k\alpha_1$ radiation, 030 reflection) on Y-cut $LiNbO_3$ substrates exchanged at: (c) 180 °C, 10 min and (d) 180 °C, 20 min in pure benzoic acid. Magnification is the same for (c) and (d).

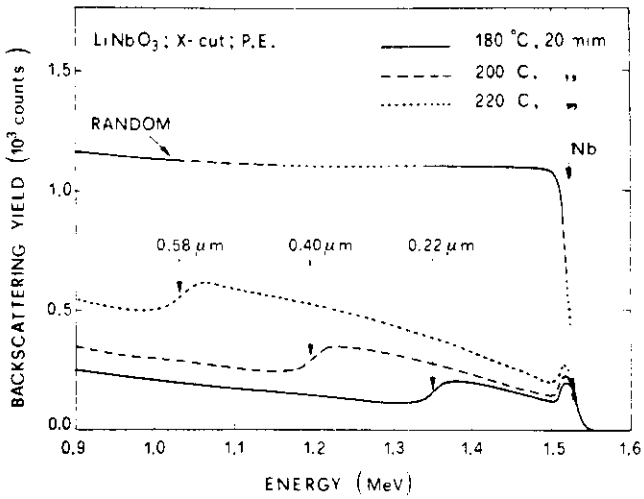


FIG. 3. Backscattering spectra in random and aligned conditions for three $X$-cut samples isochronally (20 min) exchanged at different temperatures in pure benzoic acid.

these appear as a clear peeling off of the exchange layer. Figures 2(c) and 2(d) report x-ray topographs, obtained by Lang technique in symmetric reflection geometry, taken on two $Y$-cut samples exchanged at 180 °C for 10 and 20 min, respectively. In these specimens the defects detected by XRT are dark bands aligned along the $x$ axis, the length and density of which increase with the exchange time [compare Fig. 2(c) with Fig. 2(d)] and which are clearly related to the presence of cracks observed in the SEM. It should be pointed out that XRT is much more sensitive in detecting the beginning of the surface damage and peeling-off phenomenon than is an SEM.

The mechanism of surface damage generation on $Y$-cut PE $LiNbO_3$ substrates exchanged in pure benzoic acid can be described as follows.[20] When the exchange time increases, the increasing thickness of the exchanged layer and the sharpening of its interface with the substrate lead to the generation of stress relieving defects. Remembering that the $Y$-plane is not an easy glide plane and that the temperature of the exchange process sems to be too low to favor the generation of misfit dislocations by plastic relaxation and their movement by a climb process to follow the in-depth shift of the interface, the only way to relax the high-stress gradient is through the formation of cracks. Cracks may also be observed on $Z$- and $X$-cut samples after prolonged exchange at temperatures such as 220 °C.

Exchanged samples were also examined with glancing angle x-ray diffraction using a cylindrical Wallace–Ward texture camera.[19] Diffraction patterns confirmed the presence of large strains in the exchanged layer but did not reveal the presence of any new phase, such as the cubic perovskite phase ($HNbO_3$) observed in proton exchanged $LiNbO_3$ powders.[17]

### C. Rutherford backscattering analysis

The lattice distortion induced by the proton exchange process is clearly detectable by $^4He^+$ 1.8 MeV Rutherford backscattering spectrometry[21] (RBS) in the aligned condition, thus allowing the evaluation of the thickness of the distorted layers. Figures 3 and 4 report the experimental RBS spectra taken on three $X$-cut and three $Z$-cut $LiNbO_3$ substrates exchanged for the same time, 20 min, in pure benzoic acid at three different temperatures: 180, 200, and 220 °C. Owing to the square-law dependence of the cross section on the atomic number, the RBS signal is mainly due to Nb atoms present in the target. The aligned spectra show clearly a surface region with a slightly higher backscattering yield than the virgin sample, indicating a small displacement of the Nb atoms with respect to their regular positions in the normal crystal lattice. From comparison of the spectra of Figs. 3 and 4 the displacement of Nb atoms appears to be larger along the $c$ axis than along the $a$ axis.

As shown in Figs. 3 and 4, the depth of the distorted layer clearly increased with increasing temperature when the exchange time was kept constant at 20 min. Furthermore, the small peak present at the surface for all samples

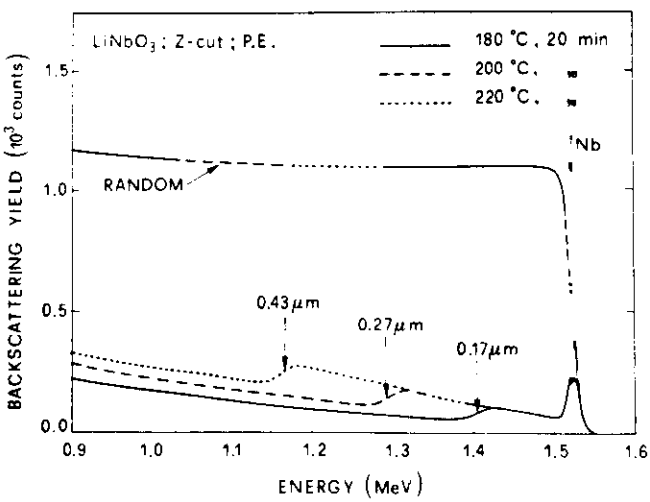


FIG. 4. Backscattering spectra in random and aligned conditions of three $Z$-cut samples isochronally (20 min) exchanged at different temperatures in pure benzoic acid.

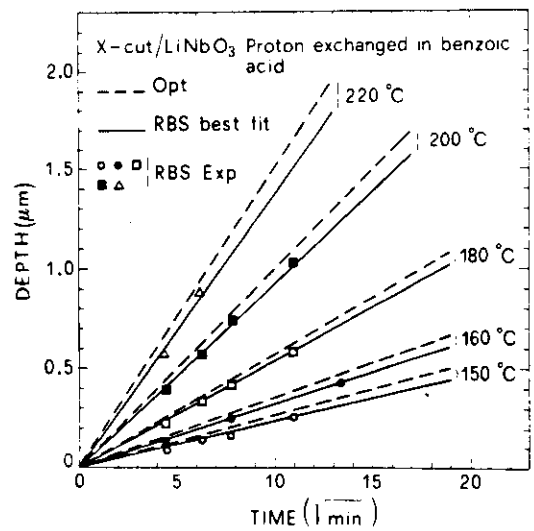


FIG. 5. Depths of exchanged regions measured by RBS in aligned conditions and by optical techniques on $X$-cut $LiNbO_3$ samples exchanged at different temperature and times in pure benzoic acid.

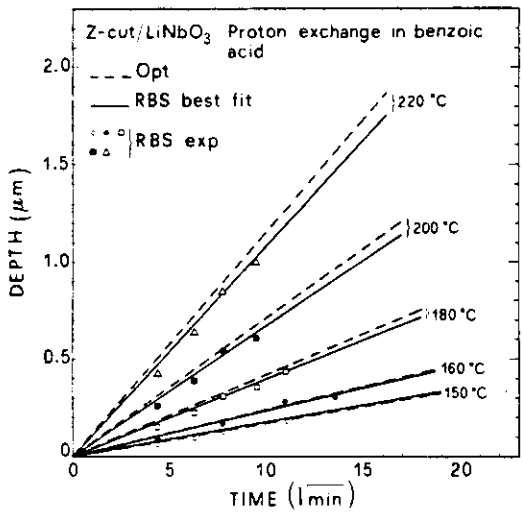


FIG. 6. Depths of exchanged regions measured by RBS in aligned conditions, and estimated from optical measurements, on $Z$-cut $LiNbO_3$ samples exchanged at different temperatures and times in pure benzoic acid.

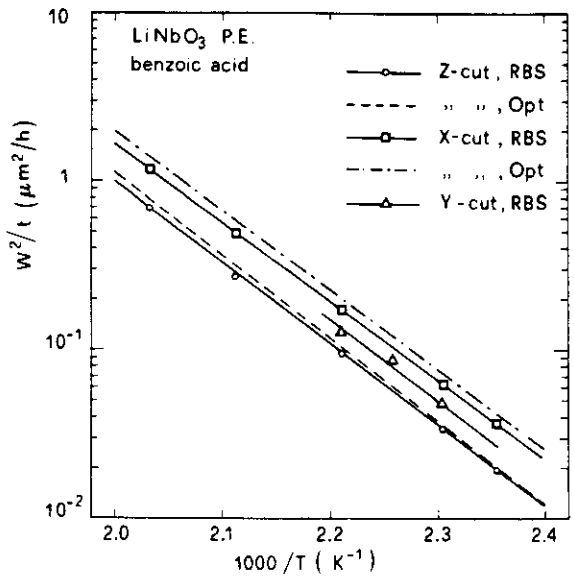


FIG. 7. $1000/T$ dependence of diffusion coefficients measured by RBS and optical techniques on $LiNbO_3$ substrates with different crystallographic orientations exchanged in pure benzoic acid.

suggests a small amount of surface damage probably caused by mechano-chemical polishing of the substrates and chemical reactions occurring at the sample surface during the exchange process.

In the random spectra, the Nb yield does not show any variation going from the exchanged surface layer to the unperturbed substrate thus suggesting that the Nb concentration remains constant across the whole sample.

Similar results have been obtained in samples exchanged at different temperatures and/or times on $Y$-cut substrates when the thickness of the exchanged layer was smaller than 2000 Å.

The thicknesses of the perturbed layers measured from the aligned RBS spectra as a function of the exchange time and temperature are shown in Figs. 5 and 6 for $X$- and $Z$-cut substrates, respectively. In all cases the measured thicknesses exhibit, at a given temperature, a square-root time dependence, indicating that the proton exchange in $LiNbO_3$ is a diffusion-limited process.

In the same Figs. 5 and 6, the waveguides depths estimated from the optical mode structure are reported for comparison. In particular the optical depths reported in Figs. 5 and 6 have been calculated from the growth data $D_0$ and $E_T$ given in Refs. 2 and 18 and obtained on multimode waveguides in order to optimize the fit of the index profile. As shown in Figs. 5 and 6 there is good agreement between depth estimates obtained from optical waveguide measurements and measurements of perturbed layer thicknesses obtained using the RBS technique. Optical depth estimates appear to be slightly ($<10\%$) higher than RBS thickness measurements.[22]

In the diffusion-controlled growth of the exchanged layer a kinetic parameter $A$ can be measured from the rate of growth of the layer, on assumption of the relation $W^2 = At$, where $W$ and $t$ are the layer thickness and time of exchange, respectively. If $A$ is taken to be the diffusion coefficient[23,24] ($D = W^2/t$) of the exchange process occurring in $LiNbO_3$ when immersed in pure benzoic acid, then the values and temperature ($T$) dependence of $D(T)$ can be obtained from the square of the slopes of the curves shown in Figs. 5 and 6.

Clearly in Fig. 7 all $D(T)$ values lie on straight and parallel lines indicating that the dependence of $D$ on temperature is given by the Arrhenius law:

$$D(T) = D_0 \exp[-(E_T/KT)],$$

with the same activation energy $E_T = 0.95$ eV. The main difference is in the absolute value of $D$ which appears larger for $X$-cut $D_{0x} = 6.09 \times 10^9$ $\mu m^2/h$, and lower for $Z$-cut $D_{0z} = 3.47 \times 10^9$ $\mu m^2/h$. The value for $Y$-cut substrates $D_{0y} = 4.93 \times 10^9$ $\mu m^2/h$, lies between these values.

### D. H and Li detection

For the analysis of H and Li which, owing to their low atomic number, are not detected by RBS with $^4He^+$ 1.8 MeV particles, two nuclear reactions (NR) have been employed. Nuclear reactions are an ion-beam technique complementary to RBS and are especially useful for the analysis of elements of low atomic number.[25] They are based on the analysis of nuclear reaction products induced by the bombarding charged particles. When the differential cross section for nuclear reaction presents a narrow isolated resonance at a well-defined value of the energy $E_R$ of the bombarding ions, the nuclear reaction which occurs is particularly suitable for atomic depth-profile measurements. On the other hand, if the differential cross section is not resonant but nearly constant or continuously varying as a function of bombarding ion energy the nuclear reaction which occurs is only suitable for determining the total amount present of the element being investigated without accurate depth resolution.

We have used a narrow isolated resonance in the reaction $^{15}N + {}^1H \rightarrow {}^{12}C + \alpha + \gamma$ which occurs at $E_R = 6.385$ MeV to measure the hydrogen content versus depth.[26] To use this resonance as probe for H, the sample is bombarded with a $^{15}N$ beam and the yield of the characteristic 4.43 MeV

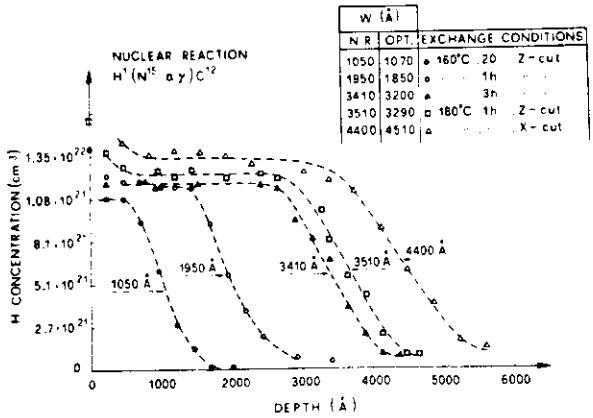


FIG. 8. Measured hydrogen profiles on $LiNbO_3$ $Z$- and $X$-cut samples exchanged in pure benzoic acid at two temperatures 160 and 180 °C and different times. The table inset compares nuclear reaction and optical measured depths.

$\gamma$ rays is measured as a function of the energy of the incident $^{15}N$ beam so that the concentration of H versus depth in the target is determined. The depth resolution of this method is finite because the resonance has a finite energy width $\pm 3$ keV, which corresponds for $LiNbO_3$ to a depth resolution of approximately 20 Å at the surface. The sensitivity of this technique for H detection is about 0.1 at. %. To avoid crystal damage and H atoms movement during the analysis the $^{15}N$ beam current density was kept lower than 10 nA/cm$^2$.

Figure 8 shows the measured hydrogen profiles in $Z$- and $X$-cut $LiNbO_3$ samples exchanged in pure benzoic acid at two temperatures, 160 and 180 °C, for several different periods. The data clearly show a steplike hydrogen distribution with a well-defined plateau where the resultant H concentration is in the range $1.1\text{–}1.3\times 10^{22}$ atoms/cm$^3$ with, apparently, a small dependence on the exchange temperature and substrate crystallographic orientation; the concentration is in fact slightly higher for $X$-cut material. The

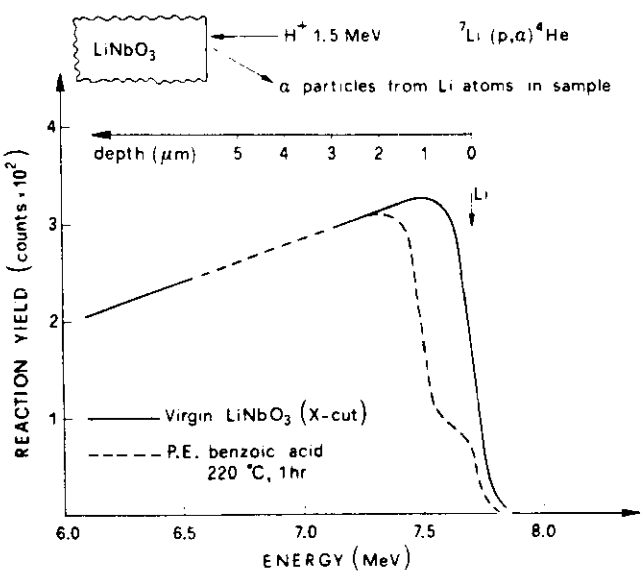


FIG. 9. $\alpha$-particle signal from $^7Li(p,\alpha)^4He$ nuclear reaction obtained on a virgin $X$-cut $LiNbO_3$ sample and on one exchanged in pure benzoic acid at 220 °C for 1 h.

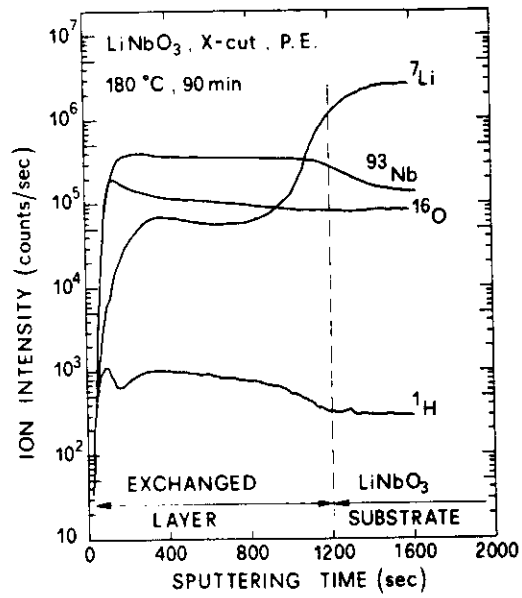


FIG. 10. $^7Li$, $^{93}Nb$, $^{16}O$, and $^1H$ intensities vs sputtering time obtained in a $LiNbO_3$, $X$-cut, sample exchanged at 180 °C, 90 min in pure benzoic acid.

depths of the exchanged region measured by nuclear reaction always agree closely with RBS data and optical measurements.

In the ion exchange process the fluxes of the two exchanging ions, $Li^+$ and $H^+$ in our case, are expected to be equal. As a consequence, from the measured concentration of H in the exchanged layer, we expect that approximately 65 to 75% of the original Li atoms present in the $LiNbO_3$ lattice have been exchanged or substituted by H atoms. To determine the proportion of Li atoms present in the exchanged layer a second nuclear reaction, $^1H + {}^7Li \rightarrow {}^4He + \alpha$, already used previously for this purpose,[27] was employed. The reaction $^1H + {}^7Li \rightarrow {}^4He + \alpha$ is not resonant so that the depth resolution achievable is quite poor, about 1000 Å. To use this nuclear reaction to detect Li, the sample is bombarded with a proton beam, having 1.5 MeV energy in our experiments, and the yield of the emerging $\alpha$ particles is measured. Figure 9 shows the $\alpha$-particle signal from Li atoms in a virgin sample and in an $X$-cut substrate exchanged at 220 °C for 1 h. The shape of the $\alpha$-particle signal produced by Li atoms in the exchanged sample clearly indicates that this sample exhibits a surface layer partially depleted of Li atoms. The thickness of this exchanged layer can be estimated from Fig. 9 approximately 1 $\mu$m in agreement with RBS data, and the concentration of Li atoms is about 30% of the original Li concentration in agreement with H profile measurements.

We have also attempted to measure atomic composition profiles in the exchanged layer with secondary ion mass spectrometry (SIMS). SIMS is in fact the only microanalytical technique suitable to detect H and Li; furthermore, SIMS has been found useful in understanding the Ti-indiffusion process in $LiNbO_3$.[28,29] However, in the case of proton exchange, the strong change of the physico-chemical properties induced by the substitution of a large fraction of the Li atoms by H atoms makes the matrix effects prevailing and the profiles consequently obtained quite unreliable. In fact

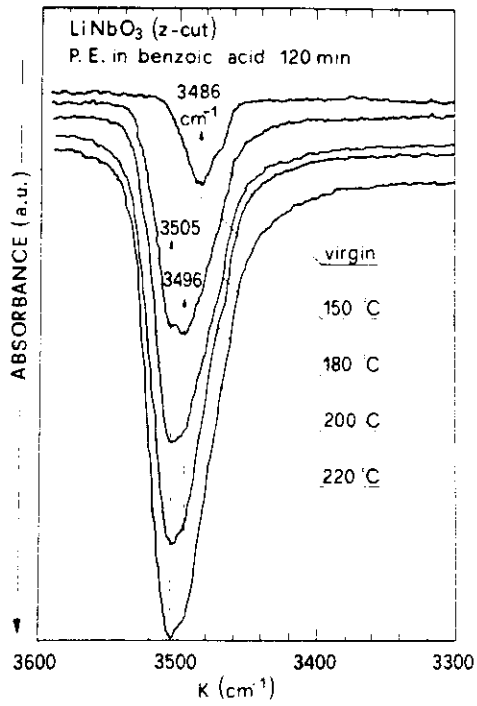


FIG. 11. IR absorbance measured in Z-cut $LiNbO_3$ samples, one virgin and the rest all exchanged for 120 min at different temperatures in pure benzoic acid.

from Fig. 10, which gives SIMS profiles obtained on an exchanged sample, an apparent increase in Nb concentration can be observed together with a decrease by a factor of 40 in the Li content in the exchanged layer with respect to the bulk. These results disagree with those obtained for Nb concentration by RBS in random conditions and with those obtained for Li content by NR and are clearly an artifact due to the matrix effect and therefore it is incorrect to compare the secondary ion intensities from the exchange layer with those from the $LiNbO_3$ substrate.

### E. Infrared absorption

Infrared transmission absorption spectra have been performed using a Perkin Elmer 180 spectrometer on samples polished on both surfaces and then proton exchanged. The results obtained are similar to those already reported in the literature.[14,17,30] In particular, the virgin sample exhibits an infrared (IR) absorption peak at 3845 $cm^{-1}$ due to OH radicals which is strongly dependent on the polarization of the incident light. The absorption peak is present for $E \perp C$ and disappears for $E \parallel C$, suggesting that the direction of the transition moment of the OH radicals is perpendicular to the $Z$ axis of the crystal.[30] After proton exchange, two absorption bands could be observed. One is a sharp and strong peak at 3505 $cm^{-1}$ which, as for the absorption peak of the virgin sample, is polarization dependent, while its intensity grows in proportion to the thickness of the exchanged layer (Fig. 11). The other is a broad, smaller, and polarization-independent absorption peak at about 3250 $cm^{-1}$.

The absorption band at about 3250 $cm^{-1}$ has been attributed to the presence of a new crystalline structure $HNbO_3$ in $LiNbO_3$ samples exchanged in pure benzoic acid.[17] We cannot confirm this hypothesis because we have been unable to detect any new structure by x-ray diffraction methods. Moreover, the high concentration of hydrogen and the considerable distortion of the crystal lattice in the exchanged layer suggest that not all the H atoms present substitute directly for Li atoms in the host lattice but that some of the H atoms may be interstitial. As a consequence the presence of two absorption peaks with different shapes and polarization dependences is more likely to be due to the different lattice positions and bondings of the H atoms present in the exchanged layer.

## IV. CONCLUSIONS

Ion-beam techniques and x-ray diffraction methods assist greatly in the characterization and understanding of the optical waveguide formation process in $LiNbO_3$ by proton exchange. In particular they can provide direct and absolute measurements of the amount and the profile of H, Li, and Nb atoms and the crystal distortion present in the exchanged layer.

In $LiNbO_3$ substrates exchanged in pure benzoic acid the H depth profile measured shows a typical steplike shape in agreement with the refractive index profile measured optically. In the constant concentration region the measured H content lies between 1.1 and $1.3 \times 10^{22}$ atoms/$cm^3$ and corresponds to an exchange of about 65–75% of the Li atoms present in the $LiNbO_3$ crystal, in broad agreement with the concentration suggested by Jackel *et al.*[12]

Measurements of the depths of the exchanged region obtained by nuclear reactions and by RBS in aligned conditions agree well with each other, proving that distortion of lattice parameters and/or atomic locations are strongly correlated to the presence of protons. Furthermore, there is good agreement between depth estimates obtained from optical waveguide measurements and measurements of exchanged layer depths obtained with ion-beam techniques.

The comparison between optical and ion-beam results provides the first direct experimental evidence that the guiding layer consists of a $LiNbO_3$ region where about 65–75% of the original Li atoms have been replaced with H atoms. This exchange apparently occurs without the formation of new phases, at least as detectable by x-ray diffraction on planar substrates. The exchange induces a large crystal distortion, sufficiently drastic to cause peeling off of the exchanged region on $Y$-cut substrates, and this may be due partially to the interstitial position of H atoms in the lattice. The large strain and disorder present in the waveguiding layer may be the reason for the large attenuation measured in these optical waveguides, while the high H atom density and the high concentration gradient at the sharp edge of the hydrogen profile may be the source of the long-term and thermal instabilities in these waveguides.

Because matrix effects prevent the meaningful use of SIMS in studying these samples we believe that ion-beam techniques together with x-ray diffraction and topography are the most suitable for the study of post annealing treatments of the exchanged waveguides[31] and the exchange processes in dilute solutions[12,31] which are reported to improve optical waveguide performances and stability.

## ACKNOWLEDGMENTS

This work was supported by Science and Engineering Research Council (U.K.) and Consiglio Nazionale delle Ricerche (Italy). We acknowledge valuable conversations with J. Winfield and the encouragement of Professor J. Lamb. A.C.G. Nutt received partial support from Barr and Strond Ltd. SIMS analyses were performed at C. Evans and Associates, San Mateo, California.

[1]J. L. Jackel, C. E. Rice, and J. J. Veselka, Appl. Phys. Lett. **41**, 607 (1982).
[2]D. F. Clark, A. C. G. Nutt, K. K. Wong, P. J. R. Laybourn, and R. M. De La Rue, J. Appl. Phys. **54**, 6218 (1983).
[3]M. De Micheli, J. Botineau, P. Sibillot, D. B. Ostrowsky, and M. Papuchon, Opt. Commun. **42**, 101 (1982).
[4]J. Noda, J. Opt. Commun. **1**, 64 (1980).
[5]E. Y. B. Pun, K. K. Wong, I. Andronovic, P. J. R. Laybourn, and R. M. De La Rue, Electron. Lett. **18**, 741 (1982).
[6]C. Warren, S. Forouhar, W. S. C. Chang, and S. K. Yao, Appl. Phys. Lett. **43**, 424 (1983).
[7]M. Papuchon and S. Vatoux, Electron. Lett. **19**, 612 (1983).
[8]K. K. Wong, R. M. De La Rue, and S. Wright, Opt. Lett. **7**, 546 (1982).
[9]M. De Micheli, J. Botineau, S. Neveu, P. Sibillot, D. B. Ostrowsky, and M. Papuchon, Opt. Lett. **8**, 116 (1983).
[10]J. L. Jackel, A. M. Glass, G. E. Peterson, C. E. Rice, D. H. Olsen, and J. J. Veselka, J. Appl. Phys. **55**, 269 (1984).
[11]A. Yi-Yan, Appl. Phys. Lett. **42**, 633 (1983).
[12]J. L. Jackel, C. E. Rice, and J. J. Veselka, Electron. Lett. **19**, 387 (1983).
[13]M. Goodwin and C. Stewert, Electron. Lett. **19**, 223 (1983).
[14]Y. Handa, M. Miyawaki, and S. Ogura, in *Processing of Guided Wave Optoelectronic Materials*, edited by R. L. Holman and D. M. Smyth, Society of Photo-Optical Instrumentation Engineers, 1984, Vol. 460, p. 101.
[15]R. A. Becker, Appl. Phys. Lett. **43**, 131 (1983).
[16]C. Canali, A. Carnera, D. Della Mea, R. M. De La Rue, A. C. G. Nutt, and J. R. Tobin, in *Processing of Guided Wave Optoelectronic Materials*, edited by R. H. Holman and D. M. Smyth, Society of Photo-Optical Instrumentation Engineers, 1984, Vol. 460, p. 49.
[17]J. L. Jackel and C. E. Rice, Ferroelectrics **38**, 801 (1981).
[18]A. C. G. Nutt, K. K. Wong, D. F. Clark, P. J. R. Laybourn, and R. M. De La Rue, *Proceedings of the 2nd European Conference on Integrated Optics*, Florence, Oct. 1983 (IEE Conference London, 1983), No. 227, p. 53.
[19]C. A. Wallace and R. C. C. Ward, J. Appl. Crystallogr. **8**, 255 (1975), **8**, 545 (1975).
[20]S. M. Al-Shukri, A. Dawar, R. M. De La Rue, A. C. G. Nutt, A. Campari, C. Ferrari, G. Mazzi, and C. Summonte, J. Appl. Phys. (to be published).
[21]W. K. Chu, J. W. Mayer, and M. A. Nicolet, *Backscattering Spectrometry* (Academic, New York, 1978).
[22]The disagreement of 30% between optical and RBS measurements for *X*-cut substrates, reported in Ref. 16 together with preliminary results of this work, was due to an error in the exchange temperature of one series of samples.
[23]K. N. Tu and J. W. Mayer, in *Thin Films: Interdiffusion and Reactions*, edited by J. M. Poate, K. N. Tu, and J. W. Mayer (Wiley, New York, 1978), Chap. 10.
[24]Since the proton exchanged layer is a uniform layer whose thickness grows with a $\sqrt{t}$, we prefer to take $D = W^2/t$, as taken in silicide studies, and not $D = 4W^2/t$, as taken for simple diffusion profiles as in Ti:$LiNbO_3$ waveguides.
[25]P. Mazzoldi and G. Della Mea, Thin Solid Films **77**,181 (1981).
[26]W. A. Lanford, Nucl. Instrum. Methods **149**, 1 (1978).
[27]Yi-Xin Chen, W. S. C. Chang, S. S. Lau, L. Wielunski, and R. L. Holman, Appl. Phys. Lett. **40**, 10 (1982).
[28]M. N. Armenise, C. Canali, M. De Sario, A. Carnera, P. Mazzoldi, and G. Celotti, J. Appl. Phys. **54**, 62 (1983); **54**, 6223 (1983).
[29]M. De Sario, M. N. Armenise, C. Canali, A. Carnera, P. Mazzoldi, and G. Celotti, J. Appl. Phys. **57**, 1482 (1985).
[30]J. R. Harrington, B. Dischler, A. Räuber, and J. Schneider, Solid State Commun. **12**, 351 (1973).
[31]J. L. Jackel and C. E. Rice, in *Processing of Guided Wave Optoelectronic Materials*, edited by R. L. Holman and D. M. Smyth, Society of Photo-Optical Instrumentation Engineers, 1984, Vol. 460, p. 43.